Available online at www.sciencedirect.com

ScienceDirect

IFAC PapersOnLine 53-5 (2020) 560–565

Uncalibrated Image-Based Visual Servoing Control with Maximum Correntropy Kalman Filter

Ren Xiaolin[1,2,3], Li Hongwen[1,2]

[1]*University of Chinese Academy of Sciences, Beijing, China*
[2]*Changchun Institute of Optics and Fine Mechanic and Physics, Chinese Academy of Science, Changchun, China*
[3]*School of Electrical & Electronic Engineering, Changchun University of Technology, Changchun, China*
(e-mail:xlren1985@ccut.edu.cn; e-mail: lihongwen@ciomp.ac.cn)

Abstract: A major challenge in solving robot visual servoing problems with unstructured environments is to obtain image Jacobian matrix, especially non-Gaussian noise always exist in the whole process. However, the standard Kalman Filter (KF) is exhausted to find the optimal value under Gaussian noise assumption. In this paper, a Kalman filter which adopted the maximum correntropy criterion (MCC) instead of the minimum mean square error (MMSE) criterion is proposed to solve the approximation issue of the image Jacobian. The simulation and experiment results using a conventional 6R manipulator are conducted to verify the effectiveness of the proposed method.

Keywords: Visual servoing, Image Jacobian matrix, Kalman filter, Maximum correntropy criterion, non-Gaussian noise

1. INTRODUCTION

Utilizing visual feedback signals has been used as a meaningful technique in robotic industry to implement the positioning or motion control especially in unstructured environments. Visual servoing makes use of visual feature information of the target object to calculate the robot control law so as to converge to an allowable error domain. According to the representation form of the signal value returned by visual feedback, it can be divided into position-based visual servoing (PBVS), image-based visual servoing (IBVS) and hybrid visual servo control system (Chaumette & Hutchinson, 2006; Chaumette & Hutchinson, 2007 Hutchinson, S., Hager, G.D., Corke, & P.I., 1996). The one type of IBVS, which is considered as uncalibrated IBVS, does not require scene model or camera/robot calibration (Kosmopoulos,2011). It uses parameter estimation to identify the unknown camera parameters, and then designs the controller based on the identified Jacobian matrix to obtain the best performance (Tao, Gong & Ding, 2016). It is important to note that uncalibrated-based methods are active research areas.

For kinematic uncalibrated visual servo, the design of its control law is most attention to the issue of the interaction matrix. The running process not only contains uncertainty of model and parameters, but also is affected by noise and external interference. Some existing works on Jacobian matrix have been reported based on nonlinear optimization and state estimation methods, such as Broyden and its improvements method (J. A. Piepmeier, G. V. Mcmurray, and H. Lipkin, 1999; Music, J. , Bonkovic, M. , & Cecić, M., 2014; M. Hao and Z. Sun,2012), recursive least squares (J. A. Piepmeier, H. Lipkin, 2002), Levenberg-Marquadt (J.M. Sebastian, Pari L, Angel Let al, 2009),Kalman filter (KF) (J. Qian and J. Su, 2002), and particle filtering (PF) (J. Ma, Q. Zhao, 2012). Music et al. (Music, J. , Bonkovic, M. , & Cecić, M., 2014) systematically compared dynamic Broyden-Gauss-Newton method, group-based Broyden method, KF method and PF method, and summarized that these algorithms have their own short comings in calculating speed or dealing with environmental noise. Support vector regression (SVR) was used to map each feature component of joint angle nonlinearly to the image feature space, construct a support vector regression machine for each joint angle, and then obtain the expression of image Jacobian matrix in Li Hexi, Shi Yonghua, Wang Guorong (2013). It is presented a method for MAP estimation of unknown noise statistics information in Liu Song Qing and Liu Shi Yue (2015). In order to improve the accuracy of estimation, fuzzy adaptive KF is used to adjust noise information based on the match technique of the filter residual mean value and covariance error (Lv, X. , & Huang, X.,2007). Zhong et al. proposed an algorithm combining robust Kalman filtering with Elman Neural Network, which using image features as input to identify the interaction matrix online (Zhong, Zhong & Peng, ,2013). In their recent studies, they used neural network filtering approach based on Kalman filtering to minimize estimation error of the interaction matrix approximation, while the non-Gaussian noises are ignoring (Zhong, X. , Zhong, X. , & Peng, X., 2015; Zhong, X. , Zhong, X. , Hu, H. , & Peng, X., 2019).

The aim of this paper is to improve the robustness of visual servoing system when the noise is non-Gaussian assumption.

10.1016/j.ifacol.2021.04.200

The KF based on MCC is employed to estimate the image Jacobian matrix.

The organization of this paper is as follows: Section 2 describes the principle of IBVS for Robotic Manipulator. The visual servoing controller based on I-ELM and adaptive gain is introduced in Section 3. And simulations on an eye-in-hand 6DOF robot are illustrated in Section 4 to show the effectiveness of the proposed approach. Finally, conclusions are given in the last section.

2. THE PRINCIPLE OF IBVS FOR ROBOTIC MANIPULATOR

In this paper, an eye-in-hand configuration is used to robot manipulator. The visual servoing control is to actuate the robot end-effector together with camera towards desired image features through robot joint motions. The image features may be directly used for control purposes, and the image space error $e(k)$ at epoch t is formed as:

$$e(k) = f(k) - f^* \tag{1}$$

where $f(k) = [f_1(k), \cdots, f_m(k)]^T \in \mathbb{R}^{m\times 1}$ is the vector of image features at time k, m is the number of image features, f^* is the desired vector of features.

Let $p(k) = [p_1(k), \cdots, p_n(k)]^T \in \mathbb{R}^{n\times 1}$ represent the robot end-effector pose in the task space, $n = 6$ is the dimension of vector, $\dot{p}(k)$ can be expressed the corresponding velocity screw. The general approach is to describe the relationship between the image feature and the robot end-effector velocity, given by the equation

$$\dot{f}(k) = J_{image}(k) \cdot \dot{p}(k) \tag{2}$$

where $J_{image}(k)$ is image Jacobian matrix (or interaction matrix), it can be denoted as follows:

$$\begin{aligned} J_{image}(k) &= \frac{\partial f(k)}{\partial p(k)} \\ &= \begin{bmatrix} \frac{\partial f_1(k)}{\partial p_1(k)} & \cdots & \frac{\partial f_1(k)}{\partial p_n(k)} \\ \vdots & \ddots & \vdots \\ \frac{\partial f_m(k)}{\partial p_1(k)} & \cdots & \frac{\partial f_m(k)}{\partial p_n(k)} \end{bmatrix}_{m\times n} \\ &= \begin{bmatrix} j_{11} & \cdots & j_{1n} \\ \vdots & \ddots & \vdots \\ j_{m1} & \cdots & j_{mn} \end{bmatrix}_{m\times n} \end{aligned} \tag{3}$$

In order to actuate a robot from the current pose to the desired pose, the most approach is using of a proportional control:

$$u(k) = \dot{p}(k) = -\lambda \cdot J_{image}{}^{+}(k) \cdot e(k) \tag{4}$$

Where $u(k)$ is control input, $J_{image}{}^{+}(k)$ is the pseudo-inverse of image Jacobian matrix, and scale factor λ is a gain constant.

3. MAXIMUM CORRENTROPY CRITERION KALMAN FILTER WITH NON-GAUSSIAN NOISE

3.1 Kalman Filter

Kalman Filter for image Jacobian identification requires a discrete linear dynamics system. The state equation of discrete-time dynamical system can be expressed as:

$$X(k) = AX(k-1) + q(k) \tag{5}$$

where $X(k) = [j_{11}, \cdots, j_{mn}]^T \in \mathbb{R}^{mn\times 1}$ is the state vector, $q(k) \in \mathbb{R}^{mn\times 1}$ is the system model noise, A is the state transition matrix.

By discretizing (2), we can get measurement equation $Z(k) \in \mathbb{R}^{m\times 1}$,

$$Z(k) = H(k) \cdot X(k) + r(k) \tag{6}$$

where $Z(k) = f(k+1) - f(k)$ is the measurement vector, $r(k) \in \mathbb{R}^{m\times 1}$ is the measurement noise, $H(k) \in \mathbb{R}^{m\times mn}$ is the observation matrix.

$$H(k) = \begin{bmatrix} \Delta p(k) & & \\ & \ddots & \\ & & \Delta p(k) \end{bmatrix}_{m\times mn} \tag{7}$$

From equation (5) and (6), $q(k)$ and $r(k)$ are independent Gaussian white noises, their statistical characteristics are described as follow:

$$E[q(k)] = 0 \tag{8}$$

$$E[r(k)] = 0 \tag{9}$$

$$\mathrm{cov}[r(k), r(j)] = R\delta_{kj} \tag{10}$$

$$\mathrm{cov}[q(k), q(j)] = Q\delta_{kj} \tag{11}$$

$$\mathrm{cov}[q(k), r(k)] = 0 \tag{12}$$

where Q and R are the state model and measurement noise covariance matrix respectively, δ_{kj} is a Kronecker-δ function.

The state and its covariance prediction equations are

$$\hat{X}(k \mid k-1) = \hat{X}(k-1) \tag{13}$$

$$P(k \mid k-1) = P(k-1) + Q \tag{14}$$

The measurement updated equations can be written as

$$K(k) = P(k \mid k-1)H^T(k)[H(k)P(k \mid k-1)H^T(k) + R]^{-1} \tag{15}$$

$$\hat{X}(k) = \hat{X}(k \mid k-1) + K(k)[Z(k) - H(k)\hat{X}(k \mid k-1)] \tag{16}$$

$$P(k-1) = [1 - K(k)H(k)]P(k \mid k-1) \tag{17}$$

3.2 Maximum Correntropy Criterion (MCC)

Correntropy defines a novel metric that measure between two random variables. Given two random variables with $X, Y \in \mathbb{R}$, the definition of the correntropy is as follow

$$V(X,Y) = E[\kappa(X,Y)] = \int \kappa(x,y) dF_{xy}(x,y) \tag{18}$$

where E is the expectation operator, $\kappa(\cdot,\cdot)$ denotes a shift-

invariant kernel following the Mercer condition and $F_{XY}(x, y)$ is the joint distribution function of (X, Y).
In this paper, the kernel function is the Gaussian kernel:

$$\kappa(x,y) = G_\sigma(e) = \exp(-\frac{e^2}{2\sigma^2}) \tag{19}$$

where $e = x - y$ and $\sigma > 0$ denotes the kernel bandwidth.

Given a sequence of error data $\{e(i)\}_{i=1}^N$, the cost function of maximum correntropy criterion is given by

$$J_{MCC} = \frac{1}{N}\sum_{i=1}^{N} G_\sigma(e(i)) \tag{20}$$

Assume the goal is to learn a parameter vector of an adaptive model, and let $x(i)$ and $y(i)$ denote the model output and the desired response. The MCC based learning can be formulated as the following optimization problem:

$$\hat{W} = \arg\max_{W\in\Omega} \frac{1}{N}\sum_{i=1}^{N} G_\sigma(e(i)) \tag{21}$$

where $\hat{W}$ denotes the optimal solution, and Ω denotes a feasible set of parameters.

The correntropy is insensitive to large errors and hence can be used as a robust cost function in estimation related problems. (B. Chen, X. Liu, H. Zhao, and J. C. Principe,2015; Liu, X. , Chen, B. , Zhao, H. , Qin, J. , & Cao, J. . ,2017, Hou, B. , He, Z. , Zhou, X. , Zhou, H. , & Li, D. . 2017).

3.3 Kalman Filter with MCC

To improve the robustness of the visual sevroing system, the maximum correntropy Kalman filter (MCKF) is employed to deal with the estimation of image Jacobian matrix in non-Gaussian noise environments

Consider a linear system like eq. (5) and (6), the prior mean and covariance matrix are computed in eq. (13) and (14).

The MCKF algorithm can be summarized as follows:

First, choose a proper kernel bandwidth σ and a small positive threshold ε, and set

$$\begin{aligned}&\begin{bmatrix} P(k|k\text{-}1) & 0 \\ 0 & R(k) \end{bmatrix} \\ &= \begin{bmatrix} B_p(k|k-1)B_p^T(k|k-1) & 0 \\ 0 & B_r(k)B_r^T(k) \end{bmatrix} \\ &= B(k)B^T(k)\end{aligned} \tag{22}$$

and construct the following equation

$$D(k) = W(k)x(k) + e(k) \tag{23}$$

where $D(k) = B^{-1}(k)\begin{bmatrix}\hat{x}(k|k-1)\\ y(k)\end{bmatrix}$, $W(k) = B^{-1}(k)\begin{bmatrix} I \\ H(k)\end{bmatrix}$,

and then, let $t = 1$ and $\hat{x}^{(0)}(k|k) = \hat{x}(k|k-1)$, the posterior estimation is updated by the fixed-point iteration for $\hat{x}(k|k)$:

$$\hat{x}^{(t)}(k|k) = \hat{x}(k|k-1) + \tilde{K}^{(t-1)}(k)(y(k) - H(k)\hat{x}(k|k-1)) \tag{24}$$

We use eq. (24)-(30) to compute $\hat{x}(k|k)$

$$\begin{aligned}\tilde{K}^{(t-1)}(k) = \tilde{P}^{(t-1)}(k|k-1)H^T(k)\times(H(k)\tilde{P}^{(t-1)}(k|k-1)H^T(k) \\ + \tilde{R}^{(t-1)}(k))^{-1}\end{aligned} \tag{25}$$

$$\tilde{P}^{(t-1)}(k|k-1) = B_p(k|k-1)(\tilde{C}_x^{(t-1)}(k))^{-1}B_p^T(k|k-1) \tag{26}$$

$$\tilde{R}^{(t-1)}(k) = B_r(k)(\tilde{C}_y^{(t-1)}(k))^{-1}B_r^T(k) \tag{27}$$

$$\tilde{C}_x^{(t-1)}(k) = diag(G_\sigma(\tilde{e}_1^{(t-1)}(k)), \ldots, G_\sigma(\tilde{e}_n^{(t-1)}(k))) \tag{28}$$

$$\tilde{C}_y^{(t-1)}(k) = diag(G_\sigma(\tilde{e}_{n+1}^{(t-1)}(k)), \ldots, G_\sigma(\tilde{e}_{n+m}^{(t-1)}(k))) \tag{29}$$

$$\tilde{e}_i^{(t-1)}(k) = d_i(k) - w_i(k)\hat{x}^{(t-1)}(k|k) \tag{30}$$

in which $B_p(k|k-1)$ and $B_r(k)$ are obtained by Cholesky decomposition of $P(k|k-1)$ and $R(k)$, respectively, superscript (t) denotes the corresponding value, vector or matrix at the t-th iteration, $d_i(k)$ is the i-th element of $D(k)$, and $w_i(k)$ is the i-th row of $W(k)$.

when $\frac{\left\|\hat{x}^{(t)}(k|k) - \hat{x}^{(t-1)}(k|k)\right\|}{\left\|\hat{x}^{(t-1)}(k|k)\right\|} \le \varepsilon$, the iteration stops. Or iterative number reaches a preset value.
Moreover, the posterior covariance is updated by

$$\begin{aligned}P(k|k) = (I - \tilde{K}(k)H(k))P(k|k-1)(I - \tilde{K}(k)H(k))^T \\ + \tilde{K}(k)R(k)\tilde{K}^T(k)\end{aligned} \tag{31}$$

It should be noted that if the measurements are contaminated by some extremely large noises, the MCKF may face numerical problems since the matrix $\tilde{C}_y(k)$ will be nearly singular. To solve this problem, let

$$\eta(k) = y(k) - H(k)\hat{x}(k|k-1) \tag{32}$$

$$A(k) = H(k)P(k|k-1)H^T(k) + R(k) \tag{33}$$

$$v(k) = \eta^T(k)A^{-1}(k)\eta(k) \tag{34}$$

If $|v(k)| > \delta$, where $\delta > 0$ is a preset threshold, we only carry out the predict step, that is, $\hat{x}(k|k) = \hat{x}(k|k-1)$, $P(k|k) = P(k|k-1)$. If $|v(k)| \le \delta$, both the two steps will be carried out.

4. SIMULATION AND EXPERIMENTAL RESULTS

4.1 Simulation Discussions

In this section, a six-degree-of-freedom Puma560 robot is simulated. The camera is mounted on the end-effector, and the target is a static target consisting of four circular feature points. In simulation, we consider two cases of disturbances

which are Gaussian mixture noises and Gaussian noises with large outliers. The evaluation goals are test trajectory and velocity performances of KF and MCKF.

The resolution of the camera is 800×800 the coordinates of the principal point is (400,400), the focal length is 8 mm. A manual tuning for proportional gain is assumed that $\lambda = 0.5$ .The simulation model assumes that the initial joint angle of the robot is $(0, pi/4, -pi, 0, pi/4, -pi/4)$. The desired matrix of the image features is given below:

$$f^* = \begin{bmatrix} 400 & 200 & 200 & 400 \\ 400 & 400 & 600 & 600 \end{bmatrix}$$

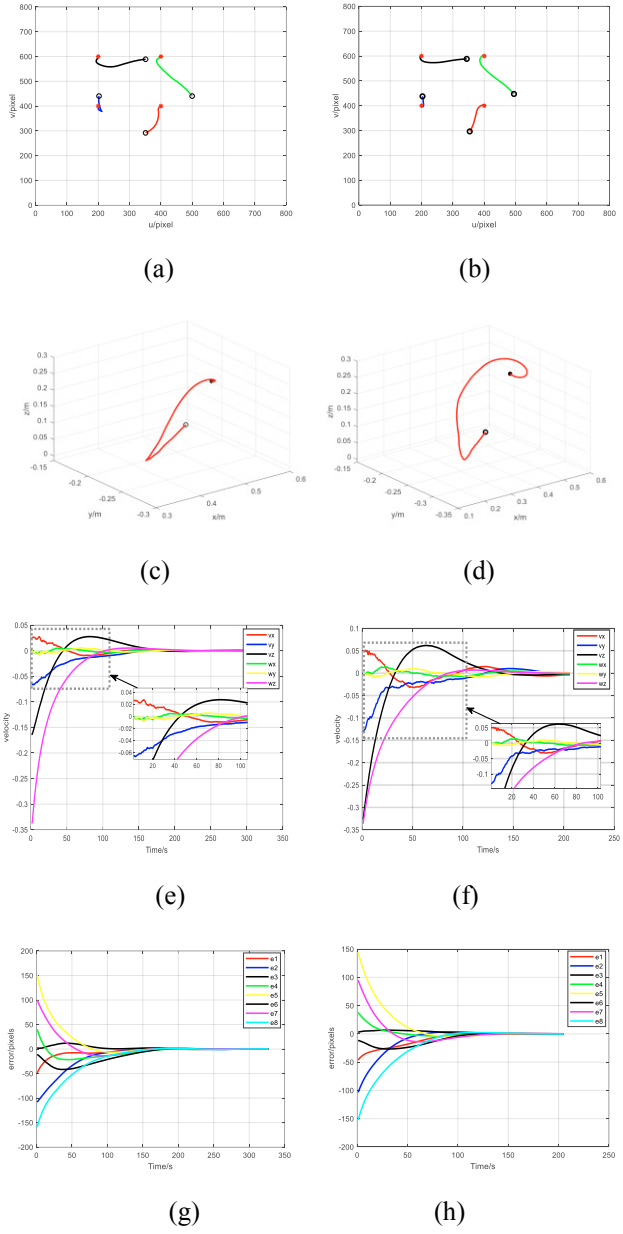

Fig. 1. Result for case 1 as 1st column for KF and 2nd column for the proposed method. (a-b) Feature trajectories, (c-d) end effector trajectories, (e-f) velocities of the end effector, (g-h) errors of the image features.

Case 1: When the image feature with Gaussian mixture noise, the results of each system for Case 1 are shown in Fig.1. The feature trajectories of the proposed method are slightly curvilinear, while the feature trajectories of KF method are obvious curvilinear as shown in Fig. 1(a-b). The end effector trajectories are smooth for both systems as shown in Fig. 1(c-d). Compare with KF method, the MCKF method performs poorly in the curvature of trajectory motion. The velocities of robot end-effector appear to vibrate slightly in both methods. The velocity performance is continuous and fast in the proposed method as shown in Fig. 1(e-f). The errors are decreasing with exponential functions of time for both systems as shown in Fig. 1 (g-h).

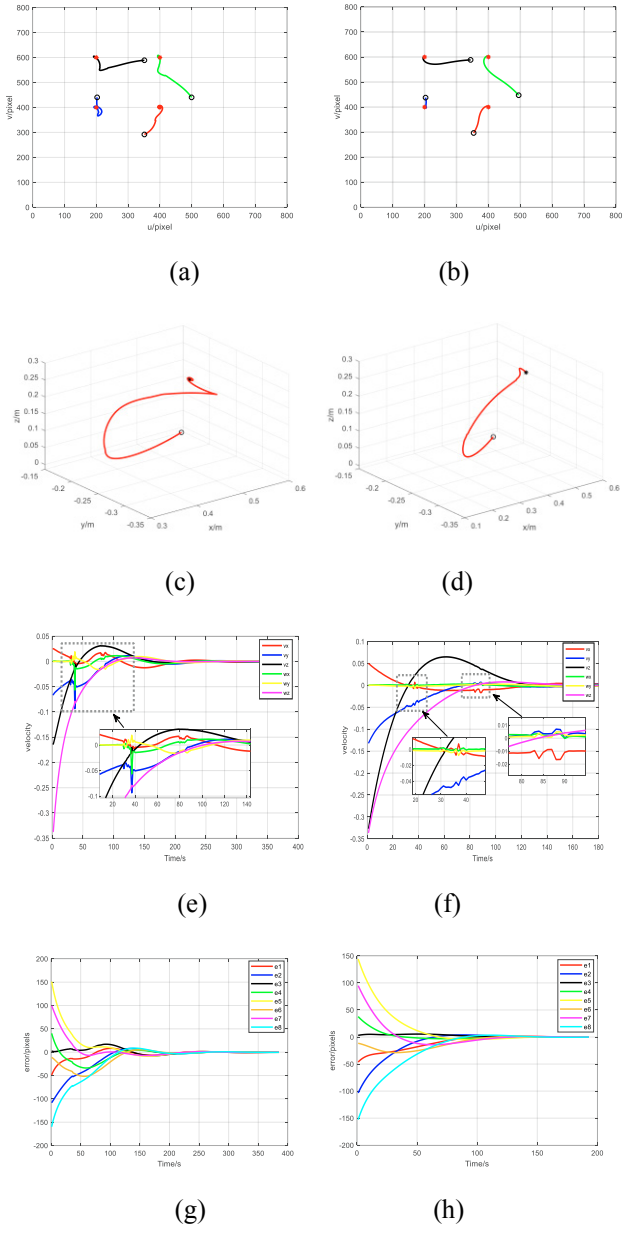

Fig. 2. Result for case 2 as 1st column for KF and 2nd column for the proposed method. (a-b) Feature trajectories, (c-d) end effector trajectories, (e-f) velocities of the end effector, (g-h) errors of the image features.

Case 2: Based on the Gaussian white noise, the original noise of 50 times is introduced into the simulation in 30-40s and

80-90s. The feature trajectories of KS method are distorted obviously by noise, the proposed method has slight chattering in movement as shown in Fig. 2(a-b). In Fig. 2(c-d), robot end-effector trajectory can move from the initial pose towards the desired pose in both methods, while the proposed method exhibit better motion effects. Compared with KF method, each element of velocity is still keeping a fast convergence rate and smaller vibration in the proposed method, as shown in Fig. 2(e-f). The proposed method produces the faster convergence rate in Fig. 2(h), meanwhile, the errors of features are decreased with exponential functions of time.

From the above simulation, it can be seen that the proposed method performs robustness of visual servoing task while the environmental noises are non-Gaussian.

4.2 Experimental Result

In the experiment, the system consists of a computer with an Intel Corei5 2.67-GHz CPU, 4GBs of RAM for image processing. and a *UR10* robotic manipulator with a Basler scA1300-32fm/fc camera mounted at its end-effector as shown in Fig. 3(a). The object is a circular target with four small black-colored circular disks of different size on the table as shown in Fig. 3(b). The object images are captured by the camera at a rate of 30 Hz. The resolution is 1280 × 1024, and the center points of the small circular disks are used as feature points.

A controller gain is $\lambda = 0.2$. The initial and desired matrix of the image features are given below:

$$f = \begin{bmatrix} 447.8 & 351.7 & 467.3 & 370.6 \\ 363.5 & 383.9 & 459.9 & 480.3 \end{bmatrix}$$

$$f^* = \begin{bmatrix} 685.1 & 588.0 & 708.9 & 611.6 \\ 496.1 & 519.5 & 593.6 & 616.9 \end{bmatrix}$$

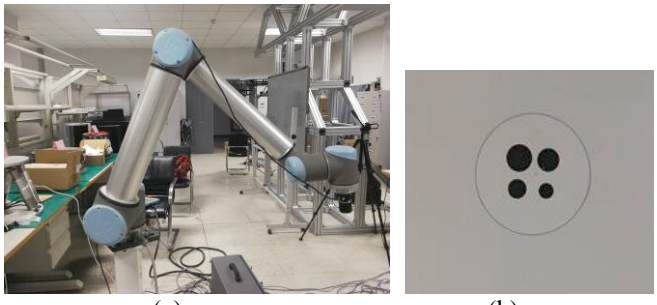

(a) (b)

Figure 3. (**a**) Experimental environment with eye-in-hand configurations. (**b**) circular target**.**

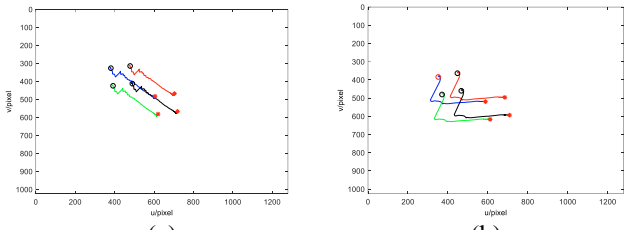

(a) (b)

Fig. 4. Experimental results for Feature trajectories. (a) the proposed method(b)KF method

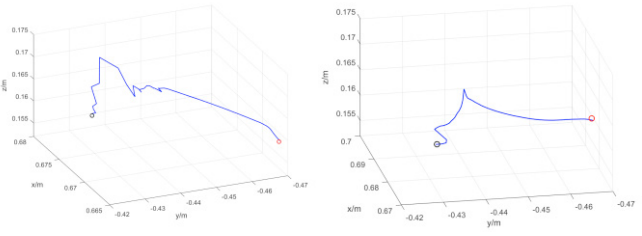

(a) (b)

Fig. 5. Experimental results for end-effector trajectories. (a) the proposed method(b)KF method

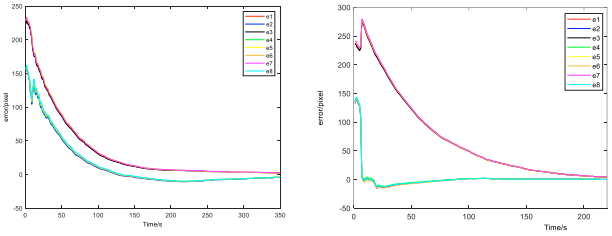

(a) (b)

Fig. 6. Experimental results for errors of the image features. (a) the proposed method(b)KF method

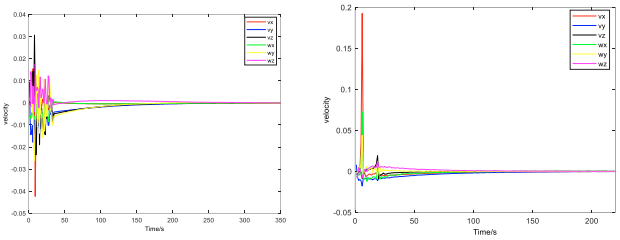

(a) (b)

Fig. 7. Experimental results for velocities of the end effector. (a) the proposed method(b)KF method

The feature trajectories of the proposed method are nearly linear and slightly vibration, while the feature trajectories of KF method are not linear as shown in Fig. 4. Both of the end-effector trajectories have unnecessary retreat and vibration as shown in Fig. 5. Fig. 6(a) and (b) show that errors of image features are gradually reduced to desired target in the allowable error domain. However, the proposed method has a slower convergence rate. the velocities of robot end-effector perform vibration at the initial phase and then gradually stable in Figs.7(a) and (b). Therefore, the effectiveness of the proposed method is verified in real noisy environment.

6. CONCLUSIONS

This paper focused on the investigating the estimation of image Jacobian matrix using MCKF with non-Gaussian assumption and is better performance of feature trajectories. The system is simulated for a six-DOF robot with an eye-in-hand camera. The performance of the algorithm is demonstrated comparing with KF. The hardware implement of this algorithm in uncalibrated robotic visual servoing control is also verified. In our future work. the system will be modified according to camera retreat

ACKNOWLEDGMENT

This work is supported by the National Natural Science Foundation of China (Grant no. 61773075 and 61703055), the Scientific Technological Development Plan Project in Jilin Province of China (Grant nos. 20200801056GH and 20190103004JH) and the Science and Technology project of Jilin Provincial Education Department of China during the 13th Five-Year Plan Period (JJKH20200672KJ, JJKH20200673KJ and JJKH20200674KJ).

REFERENCES

B. Chen, X. Liu, H. Zhao, and J. C. Principe(2015).Maximum correntropy Kalman filter, Automatica, 76, 70-77.

Chaumette, F. , & Hutchinson, S. . (2006). Visual servo control. I. basic approaches. IEEE Robotics & Automation Magazine, 13, 82-90.

Chaumette, F. , & Hutchinson, S. . (2007). Visual servo control. II. advanced approaches [tutorial]. IEEE Robotics & Automation Magazine, 14(1), 109-118.

Hao, M. , & Sun, Z. . (2012). A universal state-space approach to uncalibrated model-free visual servoing. IEEE/ASME Transactions on Mechatronics, 17(5), 833-846.

Hou, B. , He, Z. , Zhou, X. , Zhou, H. , & Li, D. . (2017). Maximum correntropy criterion kalman filter for α -jerk tracking model with non-gaussian noise. Entropy, 19(12), 648.

Huang, G. , Huang, G. B. , Song, S. , & You, K. . (2015). Trends in extreme learning machines: a review. Neural Networks, 61, 32-48.

Hutchinson, S., Hager, G.D., Corke, & P.I. (1996). A tutorial on visual servo control. Robotics & Automation IEEE Transactions on, 12(5),651-670.

Jie Ma, & Qingjie Zhao. (2012). Robot visual servo with fuzzy particle filter. Journal of Computers, 7(4).

J.M. Sebastián, Pari, L. , Angel, L. , & Traslosheros, A. . (2009). Uncalibrated visual servoing using the fundamental matrix. Robotics & Autonomous Systems, 57(1), 1-10.

Kosmopoulos, D. I. . (2011). Robust jacobian matrix estimation for image-based visual servoing. Robotics & Computer Integrated Manufacturing, 27(1), 82-87.

Li Hexi, Shi Yonghua, Wang Guorong. (2013). Vision-guided welding robot based on SVR-Jacobian estimator. Journal of South China University of Technology (Natural Science Edition), 041(007):19-25.

Liu, X. , Chen, B. , Zhao, H. , Qin, J. , & Cao, J. . (2017). Maximum correntropy kalman filter with state constraints. IEEE Access,5, 25846-25853.

Lv, X. , & Huang, X. . (2007). Fuzzy Adaptive Kalman Filtering based Estimation of Image Jacobian for Uncalibrated Visual Servoing. IEEE/RSJ International Conference on Intelligent Robots & Systems. IEEE.

Mansard, N. , & Chaumette, F. . (2007). Task sequencing for high-level sensor-based control. IEEE Transactions on Robotics, 23(1), 60-72.

Music, J. , Bonkovic, M. , & Cecić, M. . (2014). Comparison of uncalibrated model-free visual servoing methods for small-amplitude movements: a simulation study. International Journal of Advanced Robotic Systems, 11, 187-194.

Piepmeier, J. A. , B.A. Gumpert, & Lipkin, H. . (2002). Uncalibrated Eye-in-Hand Visual Servoing. Robotics and Automation, 2002. Proceedings. ICRA '02. IEEE International Conference on. IEEE.

Piepmeier, J. A. , Mcmurray, G. V. , & Lipkin, H. . (2008). A dynamic quasi-Newton method for uncalibrated visual servoing. IEEE International Conference on Robotics & Automation. IEEE.

Qian, J. , & Su, J. . (2002). Online estimation of image Jacobian matrix by Kalman-Bucy filter for uncalibrated stereo vision feedback. IEEE International Conference on Robotics & Automation. IEEE Xplore.

Qing, L. S. , & Yue, L. S. . (2015). Online-estimation of Image Jacobian based on adaptive Kalman filter. 2015 34th Chinese Control Conference (CCC). IEEE.

Tao Bo, Gong Zeyu, Ding Han.(2016) Survey on Uncalibrated Robot Visual Servoing Control. Chinese Journal of Theoretical and Applied Mechani, 48(4),767-783.

Zhong, Xungao, Zhong, Xunyu, Peng, Xiafu. (2013). Robust Kalman Filtering Cooperated Elman Neural Network Learning for Vision-Sensing-Based Robotic Manipulation with Global Stability. Sensors, 13(10):13464-13486.

Zhong, X. , Zhong, X. , & Peng, X. . (2015). Robots visual servo control with features constraint employing kalman-neural-network filtering scheme. Neurocomputing, 151, 268-277.

Zhong, X. , Zhong, X. , Hu, H. , & Peng, X. . (2019). Adaptive neuro-filtering based visual servo control of a robotic manipulator. IEEE Access,7, 76891-76901.